

UC San Diego

UC San Diego Previously Published Works

Title

Reduced apoptosis in Chinese hamster ovary cells via optimized CRISPR interference

Permalink

<https://escholarship.org/uc/item/1r8120gw>

Journal

Biotechnology and Bioengineering, 116(7)

ISSN

0006-3592

Authors

Xiong, Kai
Marquart, Kim Fabiano
Karottki, Karen Julie Cour
[et al.](#)

Publication Date

2019-07-01

DOI

10.1002/bit.26969

Peer reviewed



Published in final edited form as:

Biotechnol Bioeng. 2019 July ; 116(7): 1813–1819. doi:10.1002/bit.26969.

Reduced Apoptosis in Chinese Hamster Ovary Cells via Optimized CRISPR Interference

Kai Xiong^{1,*}, Kim Fabiano Marquart^{1,2,*}, Karen Julie la Cour Karottki^{1,*}, Shangzhong Li^{3,4,10}, Isaac Shamie^{3,10}, Jae Seong Lee⁵, Signe Gerling^{1,6}, Nan Cher Yeo⁷, Alejandro Chavez⁸, Gyun Min Lee^{1,9}, Nathan E. Lewis^{3,4,10,§}, and Helene Fastrup Kildegaard^{1,11,§}

¹The Novo Nordisk Foundation Center for Biosustainability, Technical University of Denmark, Denmark.

²Integrated Biologics Profiling/Cell line development, Novartis, Basel, Switzerland (current address).

³Department of Pediatrics, University of California, San Diego.

⁴Department of Bioengineering, University of California, San Diego.

⁵Department of Molecular Science and Technology, Ajou University, Suwon, Republic of Korea.

⁶Novo Nordisk A/S, Hillerød, Denmark

⁷Department of Pharmacology and Toxicology, Precision Medicine Institute, University of Alabama, Birmingham, USA.

⁸Department of Pathology and Cell Biology, Columbia University College of Physicians and Surgeons, New York, New York, USA.

⁹Department of Biological Sciences, KAIST, Daejeon, Republic of Korea.

¹⁰The Novo Nordisk Foundation Center for Biosustainability, University of California, San Diego, United States.

¹¹Novo Nordisk A/S, Måløv, Denmark (current address).

Abstract

Chinese hamster ovary (CHO) cells are widely used for biopharmaceutical protein production. One challenge limiting CHO cell productivity is apoptosis stemming from cellular stress during protein production. Here we applied CRISPR interference (CRISPRi) to downregulate the endogenous expression of apoptotic genes *Bak*, *Bax*, and *Casp3* in CHO cells. In addition to reduced apoptosis, mitochondrial membrane integrity was improved and the caspase activity was reduced. Moreover, we optimized the CRISPRi system to enhance the gene repression efficiency in CHO cells by testing different repressor fusion types. An improved Cas9 repressor has been identified by applying C-terminal fusion of a bipartite repressor domain, KRAB–MeCP2, to nuclease-deficient Cas9. These results collectively demonstrate that CHO cells can be rescued from cell apoptosis by targeted gene repression using the CRISPRi system.

§Correspondence to: Helene Fastrup Kildegaard (hef@biosustain.dtu.dk) and Nathan E. Lewis (nlewisres@ucsd.edu).

*These authors contributed equally to this publication.

Keywords

CHO; CRISPRi; apoptosis; mitochondrial membrane integrity; Caspase; *Bax*; *Bak*; *Casp3*

Chinese hamster ovary (CHO) cells are the most commonly used host cells for the production of therapeutic and diagnostic proteins (Walsh 2014). During protein production, metabolic stresses in CHO cells can induce apoptosis and thus reduce the viability and productivity of cells (Goswami et al. 1999). Suppressing apoptosis in CHO cell culture is therefore a crucial challenge faced by academia and industry. Under cellular stress, pro-apoptotic proteins Bak (Bcl-2 homologous antagonist/killer) and Bax (Bcl-2 associated X) are involved in permeabilization of the mitochondrial outer membrane, thus leading to release of cytochrome c (Dewson and Kluck 2009). The released cytochrome c can then activate caspases (cysteine-dependent aspartyl-specific proteases) to cleave several hundred cellular proteins for further programmed apoptosis (Dewson and Kluck 2009; Slee et al. 2001). To overcome apoptosis in CHO cells based on this known pathway, apoptosis-resistance had been shown by gene inhibition or deletion of *Bak* and *Bax* (Cost et al. 2010; Grav et al. 2015; Lim et al. 2006) as well as by gene inhibition of *Casp3* and *Casp7* (Kim and Lee 2002; Sung et al. 2007).

The CRISPR technology has emerged as an efficient method for precise genetic and translational modification. A simplified CRISPR system generally includes two components: a guide RNA (gRNA) and a Cas9 protein. The gRNA confers target specificity via DNA-RNA base-pairing and the gRNA-Cas9 complex forms to mediate DNA cleavage at the target site (Cong et al. 2013; Mali et al. 2013). Moreover, a catalytically inactive version of Cas9 (dCas9) can be generated by mutagenesis to remove the nuclease activity of Cas9. RNA-guided dCas9 can be applied to mediate gene repression by binding to the region proximate to the transcription start site (TSS) of a target gene thus blocking transcription initiation and RNA polymerase elongation (Qi et al. 2013). CRISPRi has previously been shown to repress a transgene *dhfr* (coding dihydrofolate reductase) in CHO cells to enhance protein production (Shen et al. 2017); however, the endogenous gene repression using CRISPRi in CHO cells has not yet been demonstrated.

In this study, we use CRISPRi to downregulate the endogenous expression of apoptotic genes, including *Bak*, *Bax* and *Casp3* (Figure 1a). To test the effect of CRISPRi on apoptotic genes in CHO cells, an N-terminal KRAB (Krüppel-associated box, transcription repressor) domain was fused to a CHO codon-optimized dCas9 to generate a recombinant KRAB-dCas9 repressor and three gRNA vectors were designed to target each apoptotic gene. First, in a pilot experiment (see Supplemental Figure S1), KRAB-dCas9 and the individual gRNAs were co-transfected into CHO-S cells to test all gRNAs individually or in combination. For each test, we measured the transcriptional fold change of each target gene by quantitative reverse-transcription PCR (qRT-PCR). Then, the temporal effect of CRISPRi of *Bak* and *Bax* was investigated. Collecting samples 24 hours after applying CRISPRi demonstrated the most efficient repression compared to 48 and 72 hours (Supplemental Figure S2). Based on these data, the best gRNA (gRNA3-Bak, gRNA3-Bax, gRNA1-Casp3) or a mix of all three gRNA for each gene was applied in following experiments and sampling was

performed 24 hours after transfection. As shown in Figure 1b, we further confirmed that significant gene repression of *Bak* and *Bax* mediated by CRISPRi was achieved by transfecting the gRNA mix and KRAB-dCas9; however, when we again transfected KRAB-dCas9 and each best gRNA from our pilot experiment, the CRISPRi-mediated downregulation was only evident for *Bax* (Figure 1b). In order to improve the repression efficiency of CRISPRi, we established a KRAB-dCas9-CHO cell line displaying stable and high expression of KRAB-dCas9 by precisely integrating a KRAB-dCas9 expression cassette into a transcriptionally active site (Figure 1c). This integration site was previously selected as an active genome site surrounded by highly expressing genes based on our previous study (Petersen et al. 2018). In these established KRAB-dCas9-CHO cells, CRISPRi-mediated gene repression of *Bak*, *Bax* and *Casp3* was achieved by transfecting the best gRNA. Moreover, all apoptotic genes have successfully been repressed when transfected with their respective gRNA mixes (Figure 1d). Taken together, using the combination of a gRNA mix and constitutive KRAB-dCas9 in CRISPRi displayed a more powerful repression, consistent with previous literature (Long et al. 2015). In addition, the potential of using CRISPRi for simultaneous inhibition of multiple genes (*Bak+Bax*) was also investigated in KRAB-dCas9-CHO cells; however, only *Bax* showed significant repression by CRISPRi of *Bak+Bax* combinations (Supplemental Figure S3). Correspondingly, a modest (but not significant) increase of viable cell density (VCD) was observed after the CRISPRi treatment (Supplemental Figure S4).

To investigate if CRISPRi repression of apoptotic genes can reduce the apoptosis in CHO, we transfected gRNAs targeting apoptotic genes in KRAB-dCas9-CHO cells. After 24 hours, we induced apoptosis by using Actinomycin D (ActD). 24 hours post induction, a mitochondrial potential assay was performed. In apoptotic cells, depolarized mitochondria lose the ability to aggregate JC-1 (5',6',6'-tetrachloro-1,1',3,3'-tetraethylbenzimidazolyl-carbocyanine iodide) monomers. Therefore, the ratio of JC-1 aggregates to monomers is an indicator of mitochondrial membrane integrity (Figure 2a). CCCP (Carbonyl cyanide m-chlorophenyl hydrazone), a mitochondrial membrane disruptor, was used as a positive control to fully depolarize mitochondria. As the results show, CRISPRi of *Bak* and *Bax* rescued the decreasing ratio of JC-1 aggregates to monomers after ActD induction compared with the negative control transfected with non-targeting gRNA (Figure 2b), indicating CRISPRi of apoptotic genes inhibits the depolarization of mitochondria. In addition, a caspase activity assay was performed by incubating cells with a DEVD peptide linked fluorescein (FITC). Caspase 3/7 in apoptotic cells can mediate the cleavage of the peptide and release the FITC to stain the cell DNA (Figure 2c). As expected, ActD induction enhances the caspase activity by increasing the percentage of FITC positive cells from basal levels of around 10% to around 90%; however, CRISPRi of *Casp3* decreases caspase activity in apoptotic cells by reducing FITC positive cells by ~10% (Figure 2d). In summary, CRISPRi can reduce the apoptotic phenotype in CHO cells. Along with the reduced apoptotic phenotype (Figure 2), there is an increase of VCD, albeit not significant (Supplemental Figure S5).

With the significant decrease in apoptosis and only modest increases in VCD, we wondered if the CRISPRi system could be enhanced. Although previous studies have shown that the N-terminal KRAB fusion works more effectively than a C-terminal fusion for CRISPRi in

human cells (Gilbert et al. 2014; Gilbert et al. 2013), the terminal-effects of KRAB fusion in CHO cells remained unknown. To address this, another dCas9 repression construct was designed by fusing a C-terminal KRAB to dCas9 to obtain a dCas9-KRAB construct (Figure 3a). As the results revealed by qRT-PCR (Figure 3b), C-terminal KRAB in dCas9-KRAB constructs demonstrated more efficient repression compared to KRAB-dCas9 (indicated with # in Figure 3b), which is, interestingly, in contrast to the conclusion in human cells.

We further evaluated the impact of using a second repressor domain to further enhance the suppression of apoptosis and increase VCD. Thus, we fused the C-terminal Mecp2 transcriptional repression domain (TRD) (Nan et al. 1997; Yeo et al. 2018) to dCas9-KRAB to generate a dCas9-KRAB-Mecp2 construct (Figure 3a). As predicted, the dCas9-KRAB-Mecp2 construct showed enhanced repression efficiency in 5 out of 8 cases compared to KRAB-dCas9 (indicated with # in Figure 3b) and in 4 out of 8 cases compared to dCas9-KRAB (indicated with § in Figure 3b). We thus find that all three tested CRISPRi systems could mediate the target gene repression in most cases (21 out of 24, indicated with *), albeit with different efficacies. Moreover, while the standard CRISPRi experiments only showed a modest increase in VCD (Supplementary Figure S4), the VCD after CRISPRi improved significantly when using the optimized dCas9-KRAB and dCas9-KRAB-Mecp2 constructs (Figure 3c). Notably, use of a C-terminal KRAB and fusing a Mecp2 repressor to dCas9 constructs can improve the gene repression efficiency of CRISPRi in CHO cells.

In summary, we found that CRISPRi can be successfully applied to repress endogenous expression of apoptotic genes and rescue CHO cells from cell stress induced apoptosis. Thus, the CRISPRi system joins other tools available for gene knockdowns, such as RNAi. However, CRISPRi provides unique advantages, including potentially lower off-target effects than RNAi (Boettcher and McManus 2015) and advantages in that CRISPRi suppresses transcription, while RNAi induces RNA degradation. These tools, however, will be complementary and enable pooled loss-of-function screens to identify genes associated with desired or undesirable traits, thereby guiding targeted cell line engineering. Thus, this platform enables gene function dissection and provides a new horizon for CHO cell engineering.

MATERIALS AND METHODS

gRNA design, vector construction and generation of a KRAB-dCas9-CHO cell line

gRNAs were designed to mediate CRISPRi of *Bak*, *Bax* and *Casp3* (see Supplemental Table S1 for target sequences and Supplemental Table S2 for oligos used for cloning). gRNAs were combined with either transient delivery of KRAB-dCas9, dCas9-KRAB and dCas9-KRAB-Mecp2 or delivered to cells stably expressing KRAB-dCas9 (Supplemental Figure S6). Detailed materials and methods for gRNA design, vector construction and generation of a KRAB-dCas9-CHO cell line are elaborated in supplementary information.

Cell culture, transfection and apoptosis induction

CHO-S cells (Thermo Fisher Scientific) were maintained in CD CHO medium supplemented with 8 mM L-Glutamine (Thermo Fisher Scientific) and 2 μ L/mL Anti-

Clumping reagent (AC, Life Technologies). Cells were cultivated in 125 mL Erlenmeyer shake flasks (Corning Inc., Acton, MA), incubated in a humidified incubator at 37°C, 5% CO₂ at 120 rpm and passaged every 2-3 days. One day before transfection, cells were seeded into the culture medium without AC. On the day of transfection, cells were transfected using a total amount of 3.75 µg of DNA packaged with 3.75 µL of FreeStyle Max transfection reagent (Thermo Fisher Scientific) per well of a 6-well plate (BD Biosciences) in 3 mL culture medium without AC at the adjusted density of 1.0×10^6 viable cells/mL (details about ratio of gRNA and dCas9 repressor for transfection in Supplementary table S3). All transfections were performed in biological duplicates or triplicates. To induce apoptosis, 10 µg/mL of ActD (Sigma Aldrich) was added into the culture of KRAB-dCas9-CHO cells at 24 hours after transfection with or without gRNA. 24 hours post ActD induction, cells were harvested for detection of mitochondrial membrane potential and caspase activity as described below.

Detection of mitochondrial membrane potential

For each sample, 1.0×10^6 cells were pelleted and resuspended in 1 mL warm phosphate-buffered saline (PBS, Sigma-Aldrich). For the apoptosis control, 1 µL of 50 nM CCCP was added and incubated for 5 minutes at 37 °C. 10 µL of 200 µM JC-1 was added to each sample and the cells were incubated for 30 minutes at 37 °C, 5% CO₂. After incubation, cells were washed and resuspended in PBS and measured via MACSQuant® VYB flow cytometry (Miltenyi Biotec, Bergisch Gladbach, Germany) using 488 nm excitation and 529 nm (JC-1 monomers) + 590 nm (JC-1 aggregates) emission. The ratio of JC-1 aggregates to monomers was calculated as a measure of mitochondrial membrane integrity.

Caspase activity assay

Caspase activity was detected by using CellEvent™ Caspase-3/7 Flow Cytometry Assay Kit (Life Technologies). For each sample, 1×10^6 cells were pelleted and resuspended in 1 mL warm PBS and mixed with CellEvent™ Caspase 3/7 detection reagent to a final concentration of 500 nM. After 25 minutes of incubation at 37 °C and 5 % CO₂, the SYTOX® AADvanced™ reagent was added at a final concentration of 100 µM. After an additional incubation of 5 min at 37 °C and 5 % CO₂, the percentage of FITC positive cells was measured via MACSQuant® VYB flow cytometry.

Quantitative detection of gene transcription

After CRISPRi, transcription level changes of each target gene were detected by qRT-PCR. The primers and probes for the qRT-PCR were designed using PrimerQuest™ (Integrated DNA Technologies, Coralville, IA) and listed in Supplemental Table S4. For each group 10^6 cells were spun at 200xg, supernatant was removed, and total RNA was extracted using the RNeasy Plus Mini Kit (Qiagen, Venlo, Netherlands) according to the manufacturer's instructions, followed by the quality and quantity measurement on the NanoDrop spectrophotometer 2000 (Thermo Fisher Scientific). Isolated RNA was reverse transcribed into cDNA using the Maxima First strand kit (Thermo Fisher Scientific), followed by qRT-PCR using Taqman assay in the QuantStudio 5 instrument (Applied Biosystems, Waltham, USA). Each sample had 3 technical replicates during quantification. Transcription levels of

target genes were normalized to those of *Fkbp1a* and *Gnb1* and calculated using the 2^{-Ct} method (Livak and Schmittgen 2001).

Viable cell density and viability measurement

Generally, viable cell density (VCD) and viability were monitored using the NucleoCounter NC-200 Cell Counter (ChemoMetec, Denmark). Particularly, necrosis assay was performed in Figure 3. 100 μ L cell suspension was pelleted and resuspended in 100 μ L of staining solution composed of CD CHO cell culture medium supplemented with 5 μ g/mL propidium iodide (Carl Roth, Karlsruhe, Germany). Cells were protected from light and incubated for 25 min at RT. Fluorescence assisted cell analysis was performed using a MACSQuant[®] VYB benchtop flow cytometer (Miltenyi Biotec, Bergisch Gladbach, Germany) equipped with a violet (405 nm), blue (488 nm) and yellow (561 nm) excitation laser. For each sample, a total volume of 25 μ L (approximately 20-30 k cells) was analyzed at a flow rate of 100 μ L per min. Propidium iodide positives were considered as necrotic.

Statistical analysis

Statistical analysis was performed using Microsoft Excel and GraphPad Prism. Unless otherwise stated, an unpaired two-tailed t-test was applied to determine statistical significance between independent sets of samples. The one-way analysis of variance (ANOVA) followed by a Dunnett's multiple comparison post-test was conducted for comparing more than two data sets and for many-to-one comparisons. To compare several means to each other, the Tukey's multiple comparisons test was applied. Significance was assumed for p-values less than 0.05.

Supplementary Material

Refer to Web version on PubMed Central for supplementary material.

ACKNOWLEDGEMENTS

The authors thank Nachon Charanyanonda Petersen and Karen Kathrine Brøndum for assistance with the FACS and Mads Valdemar Anderson for computational support. We acknowledge support from the Novo Nordisk Foundation (NNF10CC1016517 and NNF16OC0021638) and support from NIGMS (R35 GM119850). AC was funded by the Burroughs Wellcome Career Award for Medical Scientist. The authors declare no competing financial interests.

REFERENCES

- Boettcher M, McManus MT. 2015 Choosing the right tool for the job: RNAi, TALEN, or CRISPR. *Molecular cell* 58(4):575–585. [PubMed: 26000843]
- Cong L, Ran FA, Cox D, Lin S, Barretto R, Habib N, Hsu PD, Wu X, Jiang W, Marraffini L. 2013 Multiplex genome engineering using CRISPR/Cas systems. *Science*:1231143.
- Cost GJ, Freyvert Y, Vafiadis A, Santiago Y, Miller JC, Rebar E, Collingwood TN, Snowden A, Gregory PD. 2010 BAK and BAX deletion using zinc-finger nucleases yields apoptosis-resistant CHO cells. *Biotechnology and bioengineering* 105(2):330–340. [PubMed: 19777580]
- Dewson G, Kluck RM. 2009 Mechanisms by which Bak and Bax permeabilise mitochondria during apoptosis. *Journal of cell science* 122(16):2801–2808. [PubMed: 19795525]
- Gilbert LA, Horlbeck MA, Adamson B, Villalta JE, Chen Y, Whitehead EH, Guimaraes C, Panning B, Ploegh HL, Bassik MC. 2014 Genome-scale CRISPR-mediated control of gene repression and activation. *Cell* 159(3):647–661. [PubMed: 25307932]

- Gilbert LA, Larson MH, Morsut L, Liu Z, Brar GA, Torres SE, Stern-Ginossar N, Brandman O, Whitehead EH, Doudna JA. 2013 CRISPR-mediated modular RNA-guided regulation of transcription in eukaryotes. *Cell* 154(2):442–451. [PubMed: 23849981]
- Goswami J, Sinskey A, Steller H, Stephanopoulos G, Wang D. 1999 Apoptosis in batch cultures of Chinese hamster ovary cells. *Biotechnology and bioengineering* 62(6):632–640. [PubMed: 9951521]
- Grav LM, Lee JS, Gerling S, Kallehauge TB, Hansen AH, Kol S, Lee GM, Pedersen LE, Kildegaard HF. 2015 One-step generation of triple knockout CHO cell lines using CRISPR/Cas9 and fluorescent enrichment. *Biotechnology journal* 10(9):1446–1456. [PubMed: 25864574]
- Kim NS, Lee GM. 2002 Inhibition of sodium butyrate-induced apoptosis in recombinant Chinese hamster ovary cells by constitutively expressing antisense RNA of caspase-3. *Biotechnology and bioengineering* 78(2):217–228. [PubMed: 11870612]
- Lim SF, Chuan KH, Liu S, Loh SO, Chung BY, Ong CC, Song Z. 2006 RNAi suppression of Bax and Bak enhances viability in fed-batch cultures of CHO cells. *Metabolic engineering* 8(6):509–522. [PubMed: 16860584]
- Livak KJ, Schmittgen TD. 2001 Analysis of relative gene expression data using real-time quantitative PCR and the 2⁻CT method. *methods* 25(4):402–408. [PubMed: 11846609]
- Long L, Guo H, Yao D, Xiong K, Li Y, Liu P, Zhu Z, Liu D. 2015 Regulation of transcriptionally active genes via the catalytically inactive Cas9 in *C. elegans* and *D. rerio*. *Cell research* 25(5):638. [PubMed: 25849246]
- Mali P, Yang L, Esvelt KM, Aach J, Guell M, DiCarlo JE, Norville JE, Church GM. 2013 RNA-guided human genome engineering via Cas9. *Science* 339(6121):823–826. [PubMed: 23287722]
- Nan X, Campoy FJ, Bird A. 1997 MeCP2 is a transcriptional repressor with abundant binding sites in genomic chromatin. *Cell* 88(4):471–481. [PubMed: 9038338]
- Petersen SD, Zhang J, Lee JS, Jakobsen T, Grav LM, Kildegaard HF, Keasling JD, Jensen MK. 2018 Modular 5'-UTR hexamers for context-independent tuning of protein expression in eukaryotes. *Nucleic acids research*.
- Qi LS, Larson MH, Gilbert LA, Doudna JA, Weissman JS, Arkin AP, Lim WA. 2013 Repurposing CRISPR as an RNA-guided platform for sequence-specific control of gene expression. *Cell* 152(5):1173–1183. [PubMed: 23452860]
- Shen C-C, Sung L-Y, Lin S-Y, Lin M-W, Hu Y-C. 2017 Enhancing protein production yield from Chinese hamster ovary cells by CRISPR interference. *ACS synthetic biology* 6(8):1509–1519. [PubMed: 28418635]
- Slee EA, Adrain C, Martin SJ. 2001 Executioner caspase-3, -6, and -7 perform distinct, non-redundant roles during the demolition phase of apoptosis. *Journal of biological Chemistry* 276(10):7320–7326. [PubMed: 11058599]
- Sung YH, Lee JS, Park SH, Koo J, Lee GM. 2007 Influence of co-down-regulation of caspase-3 and caspase-7 by siRNAs on sodium butyrate-induced apoptotic cell death of Chinese hamster ovary cells producing thrombopoietin. *Metabolic engineering* 9(5-6):452–464. [PubMed: 17892962]
- Walsh G 2014 Biopharmaceutical benchmarks 2014. *Nature biotechnology* 32(10):992.
- Yeo NC, Chavez A, Lance-Byrne A, Chan Y, Menn D, Milanova D, Kuo C-C, Guo X, Sharma S, Tung A. 2018 An enhanced CRISPR repressor for targeted mammalian gene regulation. *Nature Methods*:1.

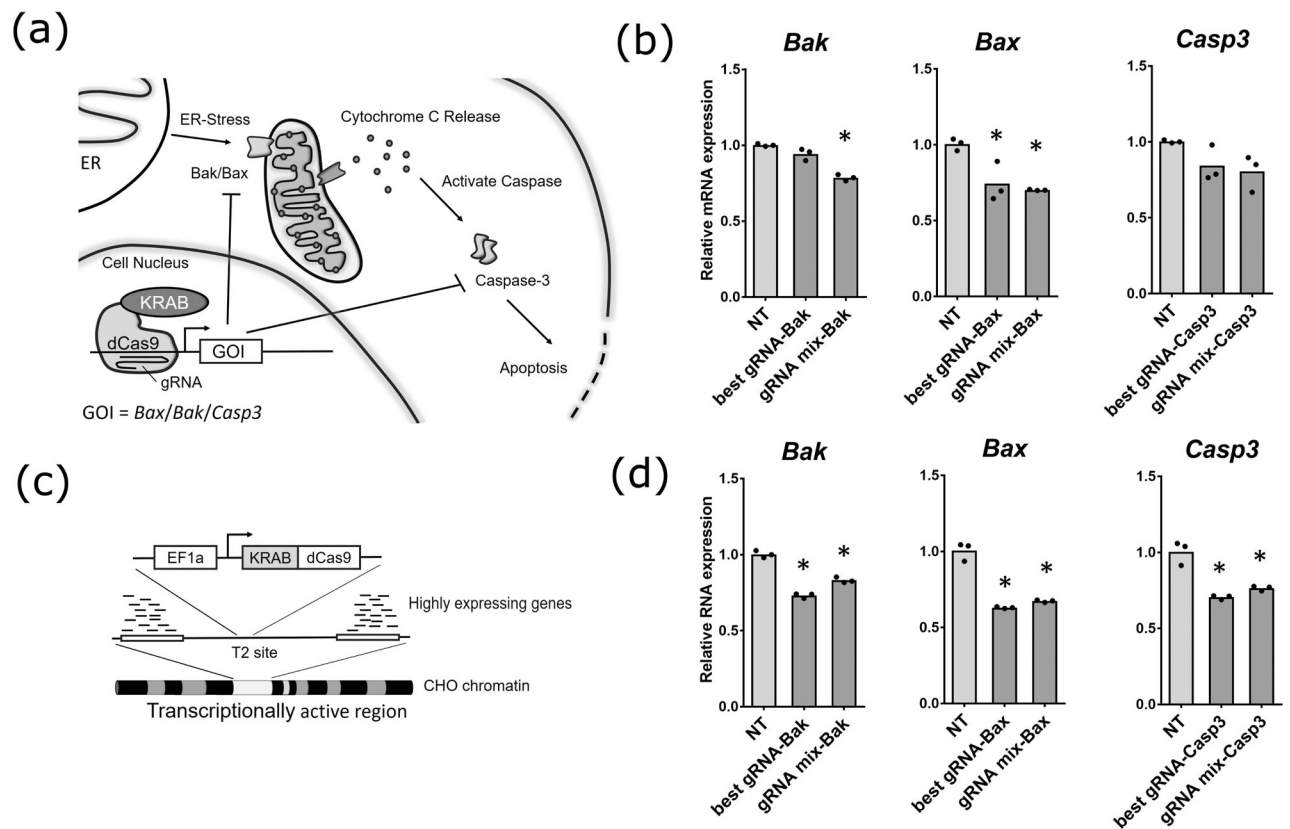


Figure 1.

Characterization of CRISPRi induced repression of apoptotic genes in CHO cells. (a) Schematic illustration of the application of CRISPRi in disrupting the apoptosis pathway in CHO cells. (b) Transcriptional repression of *Bak*, *Bax* and *Casp3* via transient expression of gRNA and KRAB-dCas9 in CHO cell measured by qRT-PCR. (c) Schematic illustration of the KRAB-dCas9-CHO cell line with precise integration of the KRAB-dCas9 expression cassette. (d) Transcriptional repression of *Bak*, *Bax* and *Casp3* via transient expression of gRNA in KRAB-dCas9-CHO cells measured by qRT-PCR. In (b) and (d), The best gRNA or the mixture of three designed gRNAs for each gene were tested in this study. mRNA was harvested 24h after transfection. NT indicates transfection with scrambled non-target gRNA and KRAB-dCas9 as a negative control. Targeted gene expression fold was shown as mean of the biological triplicates ($n=3$, * indicates $p < 0.05$ vs NT) which were normalized to *Fkbp1a* and *Gnb1* as housekeeping genes. Each transfection replicate was measured with technical triplicates of qRT-PCR. Dot represents the mean of technical triplicates in qRT-PCR.

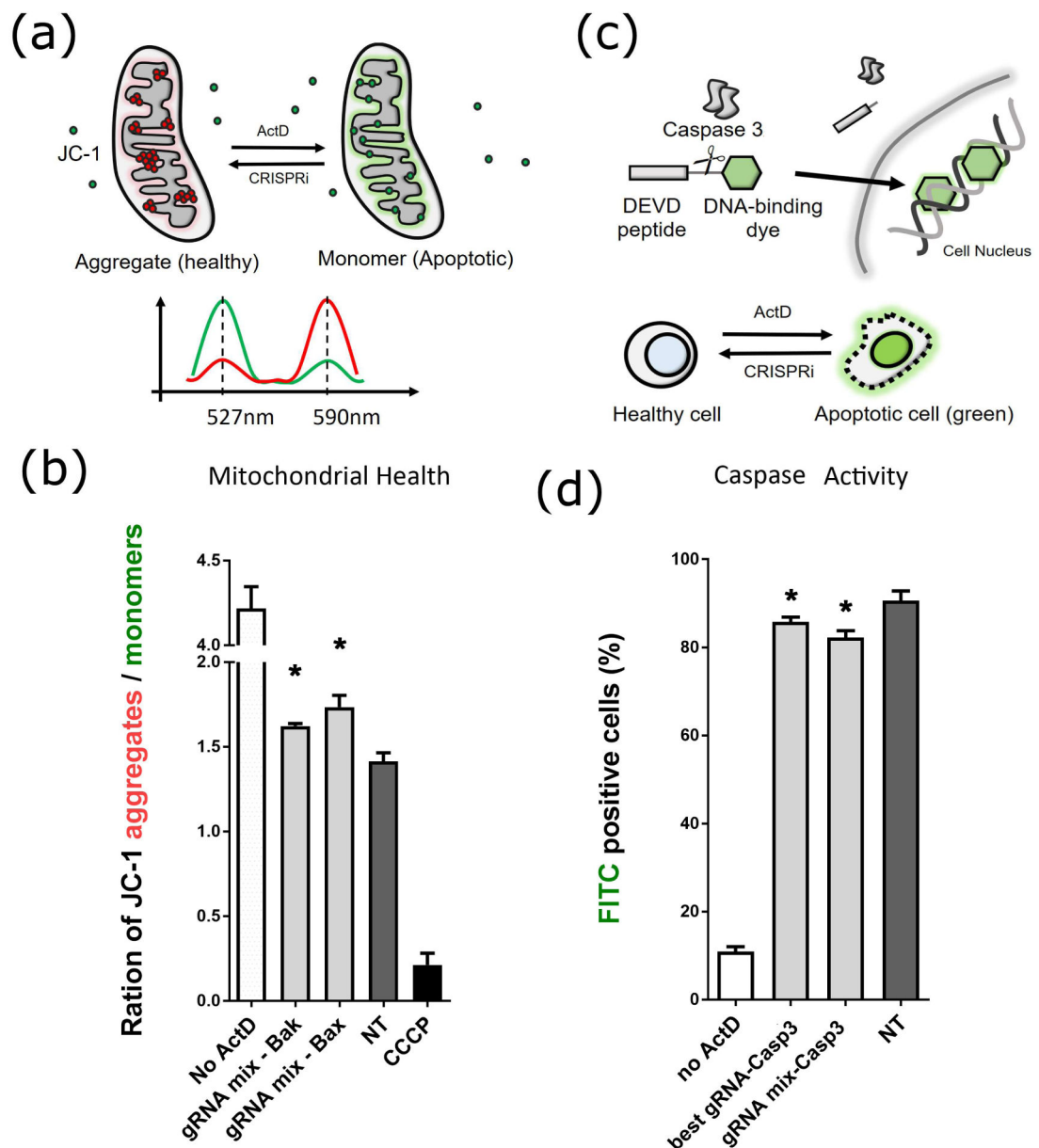


Figure 2.

Reduced apoptotic phenotype via CRISPRi. CHO apoptosis was induced by ActD 24 hours after transfection of gRNA in KRAB-dCas9-CHO cells. Another 24 hours after induction, cells were harvested and analyzed for changes in the apoptotic phenotype. (a) Schematic illustration of determination of mitochondrial membrane integrity. (b) Mitochondrial membrane integrity after CRISPRi of apoptotic genes in KRAB-dCas9-CHO cells. The mixture of three gRNAs for each gene was tested in this study. (c) Schematic illustration of caspase activity analysis. (d) Caspase activity after CRISPRi of apoptotic genes in KRAB-dCas9-CHO cells. The best gRNA or the mixture of three gRNAs for *Casp3* were tested in this study. NT represents transfection with scrambled non-target gRNA. CCCP represents carbonyl cyanide m-chlorophenyl hydrazone, a mitochondrial membrane disruptor to fully

depolarize mitochondria. Each treatment was performed in biological triplicates (n=3, * indicates $p < 0.05$ vs NT).

Author Manuscript

Author Manuscript

Author Manuscript

Author Manuscript

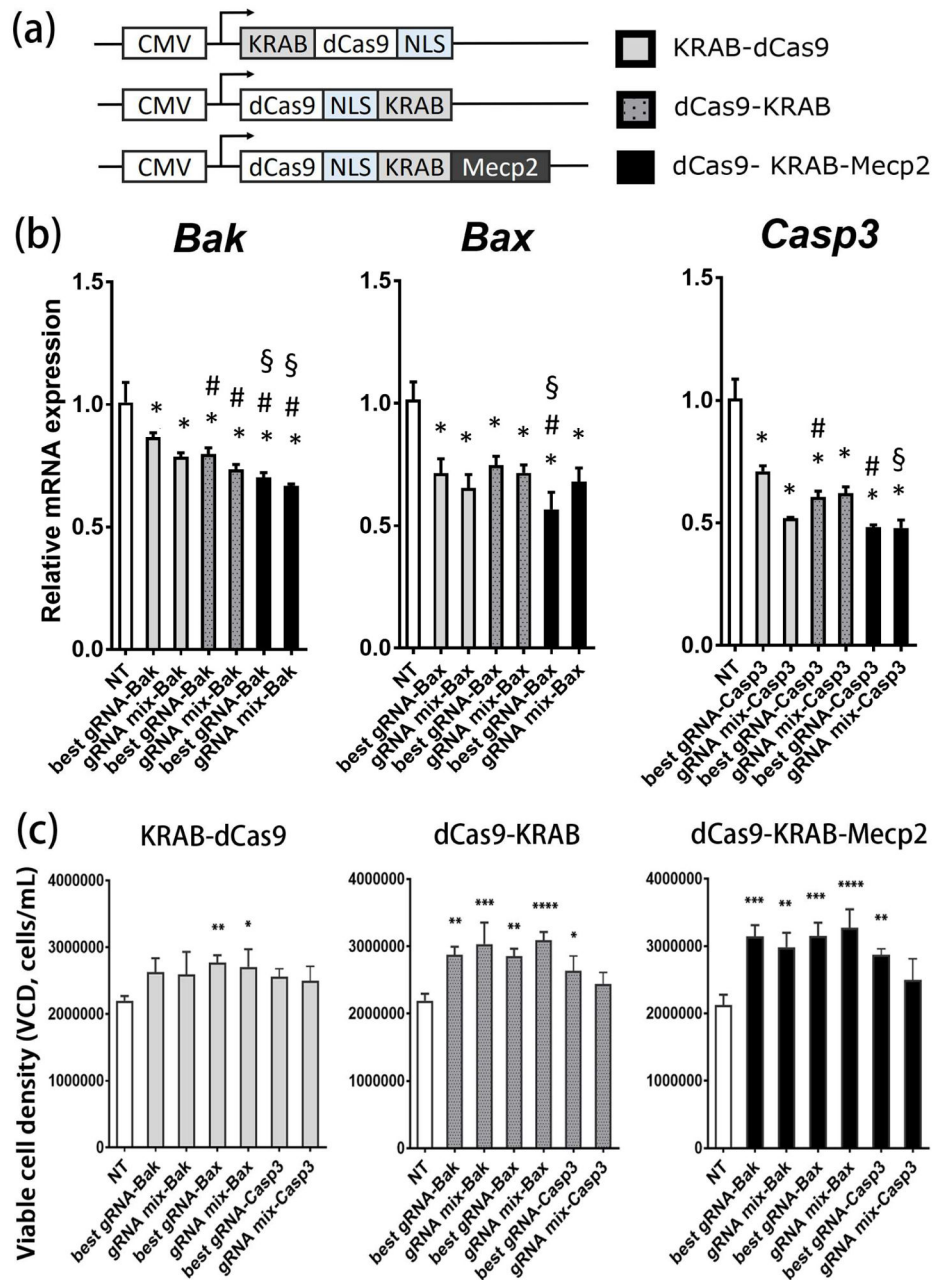


Figure 3. CRISPRi optimization in CHO cells. (a) Schematic comparison of CRISPRi vectors. NLS, nuclear localization signal; CMV, cytomegalovirus promoter; Mecp2, gene element that encodes the transcriptional repression domain of methyl CpG binding protein 2. (b) Transcriptional repression of *Bak*, *Bax* and *Casp3* via the three CRISPRi systems we tested was measured by qRT-PCR. We tested the best gRNA (gRNA3 for *Bax*, gRNA3 for *Bak*, and gRNA1 for *Casp3*) and the mixture of designed gRNAs for each gene. gRNA and dCas9-repressors were transiently co-transfected and the mRNA samples was harvested 24 hours after transfection. NT represents transfection with scrambled non-target gRNA and dCas9-KRAB-Mecp2. Targeted gene expression fold change was shown as mean of the

biological triplicates (n=3, * indicates $p < 0.05$ vs NT, # indicates $p < 0.05$ vs KRAB-dCas9, § indicates $p < 0.05$ vs dCas9-KRAB). Fold change was normalized to *Fkbp1a* and *Gnb1* as housekeeping genes. Each biological replicate was measured with technical triplicates of qRT-PCR. Error bar represents the standard deviation of transfection replicates. (c) The viable cell density of the groups in (b) was measured by flow cytometry 24 hours after transfection (n=3, * indicates $p < 0.05$ vs NT, ** indicates $p < 0.01$ vs NT, *** indicates $p < 0.001$ vs NT, **** indicates $p < 0.0001$).